electronics

MDPI

Article

An Approval of MPPT Based on PV Cell's Simplified Equivalent Circuit During Fast-Shading Conditions

Shailendra Rajput [1], Moshe Averbukh [1,*], Asher Yahalom [1] and Tatiana Minav [2]

[1] Department of Electrical and Electronics Engineering, Ariel University, Ariel 40700, Israel; shailendra.phy@gmail.com (S.R.); asya@ariel.ac.il (A.Y.)

[2] Department of Engineering and Natural Sciences, Tampere University, 33720 Tampere, Finland; tatiana.minav@tuni.fi

* Correspondence: mosheav@ariel.ac.il; Tel.: +972-528814120

Received: 1 September 2019; Accepted: 17 September 2019; Published: 19 September 2019

Abstract: The partial shading conditions significantly affect the functionality of solar power plants despite the presence of multiple maximum power point tracking systems. The primary cause of this problem is the presence of local maxima in the power–current and/or power–voltage characteristic curves that restrict the functionality of the conventional maximum power point tracking systems. The present article proposes a modified algorithm based on the simplified equivalent circuit of solar cells to improve the functionality of traditional maximum power point tracking systems. This algorithm provides a method for regularly monitoring the photo-current of each solar module. The upper and lower boundaries of the regulating parameter such as current or voltage are decided very precisely, which is helpful to find the location of the global maximum. During a sequential search, the control system accurately determines the lower and upper boundaries of the global maximum. Simultaneously, the maximum power point tracking system increases the photovoltaic current up to one of these boundaries and applies one of the conventional algorithms. Additionally, the control system regularly monitors the photovoltaic characteristics and changes the limits of regulating parameter concerning any change in global maximum location. This proposed method is fast and precise to locate the global maximum boundaries and to track global maximum even under fast-changing partial shading conditions. The improved performance and overall efficiency are validated by simulation study for variable solar irradiance.

Keywords: partial shading; solar module; maximum power point tracking; global maximum; photovoltaic system; equivalent circuit

1. Introduction

In the present century, the supply of clean, renewable, and sustainable energy is the most important technical and scientific challenge for humanity. The renewable energy resources are high in demand as the quality of human life depends to a large scale on the availability of energy. Under such circumstances, solar energy is one of the suitable choices as the solar energy resource dwarfs all other renewable and fossil-based energy resources [1]. It is a known fact that sunlight strikes Earth in 1 hour more than all the energy consumed by humans in an entire year [1]. Therefore, the global solar electricity market is rapidly growing, and its value currently is more than $10 billion/year [1–3].

The solar energy is converted to electricity directly using photovoltaic (PV) systems at the solar power plant [1]. In this decade, the PV technology market has achieved remarkable growth worldwide. This tremendous growth is related to lower investment costs, dynamic technological developments, governmental financial support, and Feed-in-Tariff [1–3]. The PV system-based power generation remains the fourth-largest renewable electricity technology in terms of generation [4]. In 2018, solar

power generation showed the largest absolute generation growth (31%) of all renewable technologies [4]. Several solar modules are linked together in series and parallel arrangements to establish a large solar plant. The maximum power point tracking (MPPT) techniques are an essential part of such solar power plants [5,6]. These systems are useful to enhance the power output of the PV systems. The primary purpose of the MPPT is to control and adjust the regulating parameter of the PV system to work on or very closely to the global maximum (GM). The target parameter can be either voltage or current of the solar penal. Generally, the current is a preferable choice as a regulating parameter because of the relative ease of control than that of voltage [6,7]. Previously, different types of modifications and embodiments of the MPPT system in the form of sequential search and by artificial control techniques are proposed and discussed [8–19]. The first group includes perturbation-observation algorithms (P&O), incremental conductance algorithms, sliding mode controllers, and many others [9–16]. The second group contains techniques related to fuzzy logic regulators [17,18]. The maximum output power of a PV system is a function of different environmental conditions such as solar radiation, partial shading, and ambient temperature. Therefore, the effect of these parameters should be considered and solved in order to achieve the maximum output power from the PV module. For instance, the partial shading conditions can occur because of weather conditions (clouds), environmental obstacles like trees and constructions, dirt, dust, bird dropping, and self-shading among PV modules caused by parallel rows. The efficiency of plants control system deteriorates because of the mismatch between voltage and current outputs of the different modules during partial shading conditions [6]. Partial shading or inhomogeneous solar irradiation of PV modules results in the formation of multiple local maxima with the GM. As a result, the MPPT system and algorithms mentioned above are unable to find the GM as they consider local maxima as a global one. If solar irradiation is changing slowly, then MPPT can scan the regulating parameter further and can search the actual GM location. However, it is challenging to locate GM in case of the rapid change in solar radiation intensity. Hence, the efficiency of the PV plant decreases significantly during the partial shading and inhomogeneous irradiation, as discussed in our previous article [19]. Previously, several naturally or bio-inspired solutions are proposed to solve this critical issue and to improve the MPPT method for partial shading or inhomogeneous irradiation conditions [20–33]. In more detail, research concentrates on various approaches such as bio-inspired algorithms [20], particle swarm optimization (PSO) algorithms [21–24], grey wolf optimization (GWO) technique [25], and simulated annealing (SA) based method [26]. Interestingly, one can obtain better results using hybrid evolutionary algorithms based on a combination of two or more different techniques. For instance, the DEPSO algorithm is a combination of the differential evolutionary (DE) and PSO algorithms [27]. As per our understanding, two-stage processes for GM search are more efficient than other approaches. In the first step, the range of regulating parameter should be determined in the vicinity of GM. Later the conventional MPPT techniques can be employed to find the exact location of the GM [28,29]. Detailed analysis of the nature-inspired MPPT algorithms for partially shaded PV systems [30], accelerated particle swarm optimization technique in [31], a modified firefly algorithm [32] and bat algorithm [33] are reported and analyzed. A special group of algorithms applies math principles based on transfer reinforcement learning approach [34] or a prediction of the GM [35] considering a pre-history of its positions. Here comes the crucial question that how precise and agile these techniques are to determine the region around the GM during the partial shading or inhomogeneous solar irradiation of PV modules [6]. For real PV systems, promising solutions are proposed to smooth the operation during partial shading conditions [36,37]. These methods are able to track the GM using relatively simple techniques. In these technologies, every PV module is attached to an individual MPPT block. However, every block's functions is related to only its PV module, hence output voltage is relatively low (~48 V). On the other hand, a single MPPT system for entire string works with much higher voltage (~1000 V and even more). Therefore, such electronic systems can be more efficient and can be able to work at higher voltage.

In this article, a two-stage search procedure is proposed to locate the GM during the partial shading and non-uniform solar radiation. The significant difference between this method and the previously

known similar methods are: (a) Module current as regulating parameter which improves the control sustainability; (b) continuous measurement of each module's voltage and current outputs; (c) applying simplified equivalent circuit of PV modules. Hence, this method is more accurate, efficient, and requires less time to search GM for fast varying environmental conditions. The paper is organized as follows; Section 2 gives a summary of the origin of multiple maxima during partial shading conditions, simplified equivalent circuit of the PV module and the proposed algorithm. This section also explains the process to find the global maximum power point (GMPP) using proposed algorithm. The third section presents simulation results as well as related discussion, and finally, the conclusions are drawn in Section 4.

2. Materials and Methods

2.1. Impact of Partial Shading on PV Characteristics

The voltage–current (*V*–*I*) and power–current (*P*–*I*) curves of a PV system under homogeneous irradiation and partial shading conditions are shown in Figure 1. The well-known PSIM software was used for simulation of both the conditions. The location of maxima in the *P*–*I* curve depends on the environmental conditions such as the intensity of solar irradiation and module temperature, which is determined using the well-known MPPT system. The *V*–*I* curve changes smoothly, and the *P*–*I* curve shows only a single maximum for uniform irradiation. In the case of partial shading conditions, the *V*–*I* curve shows step-like behavior and different maximum power points exist on the *P*–*I* curve, which results in the more complicated PV characteristics [9]. Existences of two or more maxima in the *P*–*I* curve is not suitable for the functionality of a conventional MPPT process, as discussed previously [9,19]. If the MPPT controller automatically detects local maxima during the partial shading, then the efficiency of the solar plant decreases significantly as the power at local maxima is lower than that of the global one. It is observed that more than two maxima are also possible for non-uniform solar radiation: one is GM and others are local maxima (Figure 1).

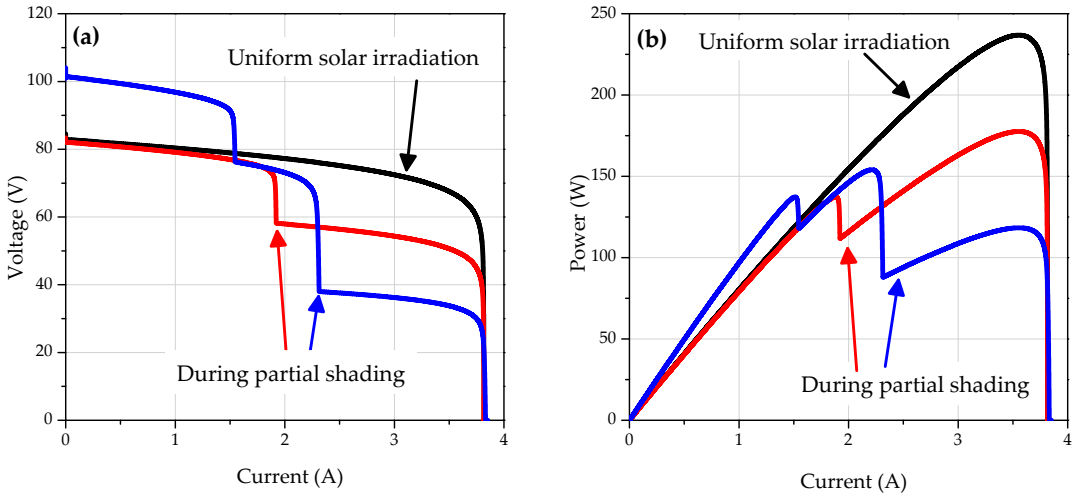

Figure 1. The (**a**) voltage–current (*V*–*I*) and (**b**) power–current (*P*–*I*) curves for under uniform irradiation and partial shading conditions.

2.2. Equivalent Circuit of the PV Module

Next, the origin of multiple local maxima under partial shading conditions is defined. Figure 2a illustrates the equivalent circuit of a solar module and electrical behavior of such a solar module is expressed as:

$$I = I_{ph} - I_0\left[exp\left(\frac{q_e V}{ak_B T}\right) - 1\right], \quad (1)$$

where I is the output current of the PV module in A, I_{ph} is the photocurrent in A, I_0 is the reverse saturation current in A, V is the output voltage in V, a is the module quality factor, k_B is the Boltzmann constant and equals to 1.3806×10^{-23} in $m^2 \cdot kg \cdot s^{-2} \cdot K^{-1}$, $q_e = 1.602 \times 10^{-19}$ is elementary charge in C, and T is the cell/module temperature. The thermal voltage ($V_T = k_B T/q$) value is equal to ~0.025 V at temperature, T = 300 K (27 °C). The I_0 reverse saturation current and a module quality factor are determined using approximating procedures from [38] in addition to the manufacturer datasheet. A set of *V–I* curves of a PV module measured under various irradiation levels and different operating temperatures can also be used for this purpose [38]. The module quality factor (a) values of silicon crystal and polycrystalline solar modules remain constant for an extensive range of temperature and solar radiation intensities [39]. Other parameters (I_{ph}, I_0, and V_T) are strongly dependent on the solar irradiation intensities and temperature changes. The reverse saturation current is expressed as [40]:

$$I_0 = I_0^* \left(\frac{T}{T_{ref}}\right)^3 exp\left\{\frac{q_e E_g}{aK_B}\left(\frac{1}{T_{ref}} - \frac{1}{T}\right)\right\}, \quad (2)$$

where T_{ref} and E_g are the reference temperature (300 K) and the bandgap of the semiconductor material, respectively. The asterisk "$*$" illustrates that the parameter value is known. The bandgap of a n numbers of serially connected silicon module solar cells is calculated as [41]:

$$E_g = n\left(1.16 - 7.02 \times 10^{-4} \frac{T^2}{T - 1108}\right). \quad (3)$$

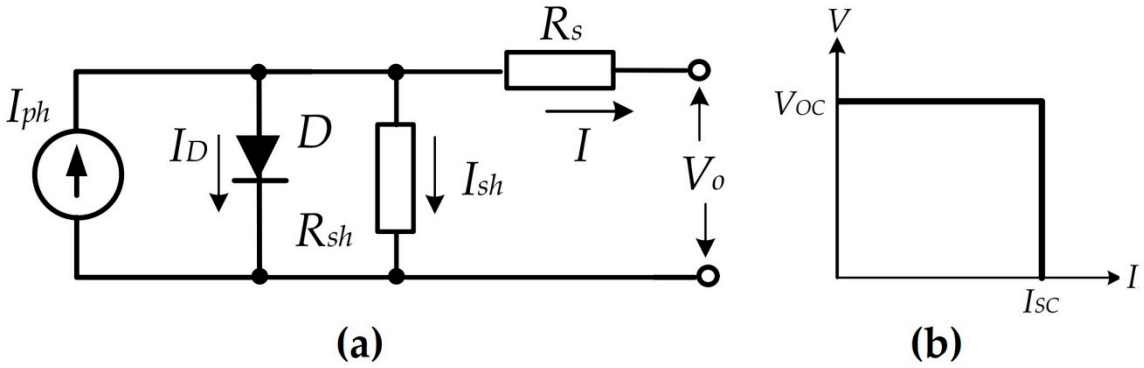

Figure 2. (**a**) The single-diode equivalent circuit of the photovoltaic cell (I_{ph} is photocurrent, D is diode, I_D is diode current, R_{sh} is shunt resistance, I_{sh} is shunt current, R_S is series resistance, I is output current, and V_0 is output voltage). (**b**) The *V–I* characteristics correspond to the simplified equivalent circuit of the solar module (V_{OC} is open-circuit voltage, I_{SC} is short-circuit current).

The photocurrent works as a current source for the PV module and supplies primary electrical energy. The relationship between photocurrent, solar irradiation level (S), and absolute temperature (J_0) is expressed as [40]:

$$I_{ph} = (I_{sc})_0 \left(\frac{S}{1000}\right) + J_0\left(T - T_{ref}\right), \quad (4)$$

where $(I_{sc})_0$ is the short-circuit current at a reference temperature. For smaller J_0 values, the photocurrent becomes closely proportional to the solar irradiation. Once all parameters of the equivalent circuit (Equation (1)) are determined, there are possibilities of different mathematical operations. For large power plants, several solar modules are connected in serial or parallel arrangements. Hence, the mathematical analysis becomes very complicated and challenging to solve with the analytical methods. This issue can be resolved by a thorough analysis of the simplified equivalent circuit of Figure 2a, as shown in our previous work [9]. The *V–I* characteristic corresponds to the simplified equivalent

circuit, as shown in Figure 2b, where V_{OC} is open-circuit voltage and I_{SC} is short-circuit current. The simplified equivalent circuit excludes both series and parallel resistances, hence, the *V–I* curve obtains the shape of a simple rectangle. The equivalent circuit model was used to calculate the parameters of the single-diode solar cell/module [38].

2.3. Localization of Global Maximum Power Point

Let us consider that the *n*-numbers of solar modules are connected serially, and every module is also associated with a parallel bypass diode (Figure 3a). It is also considered that the temperature of all modules is similar. For uniform solar radiation, these solar modules array shows a standard current and power characteristic similar to Figure 1. A simplified equivalent circuit of *n*-serially connected solar modules array was demonstrated in our previous work [9]. The open-circuit voltage $[(V_{OC})_n]$ of this array is equal to the sum of the open-circuit voltage of every module.

$$(V_{OC})_n = n \cdot V_{OC} \tag{5}$$

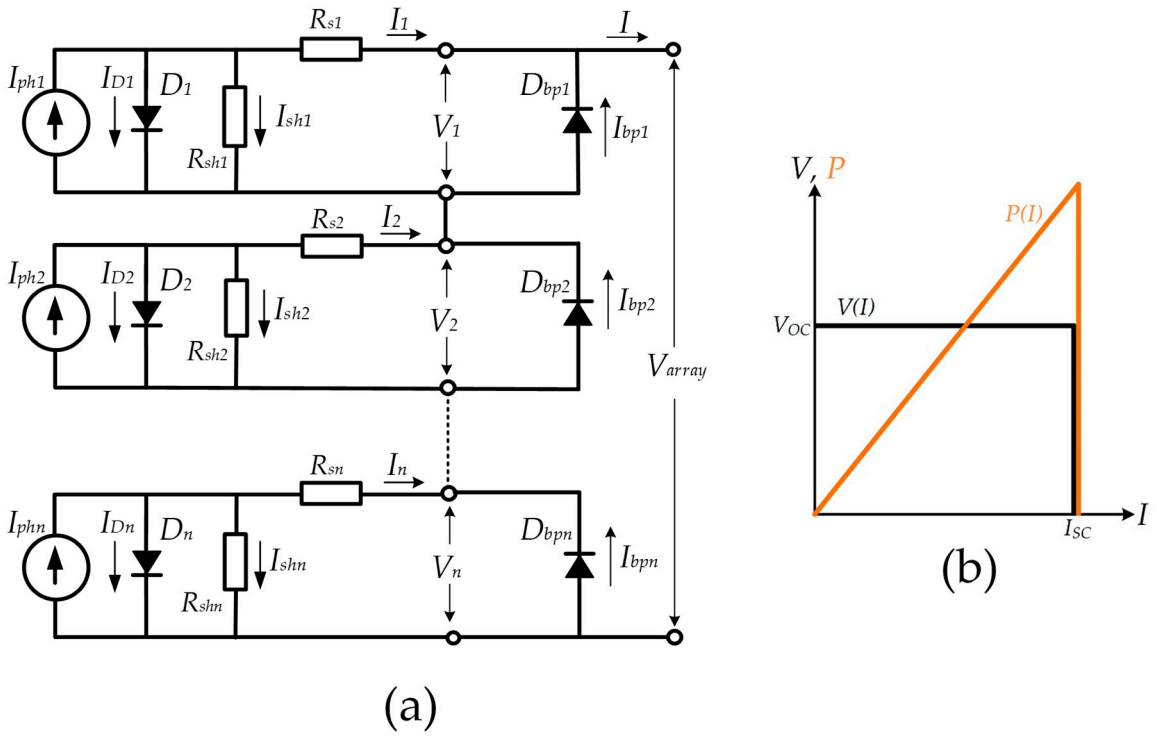

Figure 3. (**a**) The equivalent circuit of a solar array including *n*-individual solar modules with parallel bypass diodes (I_{ph1}, I_{ph2}, I_{phn} are photocurrents of PV modules; I_{D1}, I_{D2}, I_{Dn} are currents through diodes; R_{sh} is shunt resistance, I_{sh1}, I_{sh2}, I_{shn} are shunt currents; R_{S1}, R_{S2}, R_{Sn} are series resistance; D_{bp1}, D_{bp2}, D_{bpn} are bypass diodes attached to each PV module; I_{bp1}, I_{bp2}, I_{bpn} are currents through bypass diodes; V_1, V_2, V_n are output voltages PV modules; I_1, I_2, I_n are output currents of PV modules; I and V_{array} are the current and voltage of *n*-serially connected in PV modules array), (**b**) The *V–I* and *P–I* characteristic corresponds to the simplified equivalent circuit of the *n*-serially connected solar modules array (V_{OC} is open-circuit voltage and I_{SC} is short circuit current).

The short-circuit current or photovoltaic current of the array is equal to the short-circuit current of each module in case of homogeneous solar radiation on all the modules. The *V-I* and *P-I* characteristic correspond to the simplified equivalent circuit of the *n*-serially connected modules are shown in Figure 3b. Interestingly, this typical behavior changes significantly if some of the modules are irradiated with different solar intensities. In this case, the short-circuit current values of differently irradiated

modules are not the same. In order to understand this situation, let us assume that only three groups of modules are irradiated differently with respect to each other. One group of modules is irradiated more strongly than the other two remaining groups. The *V-I* and *P-I* curve for the three types of irradiation conditions are represented in Figure 4a–c.

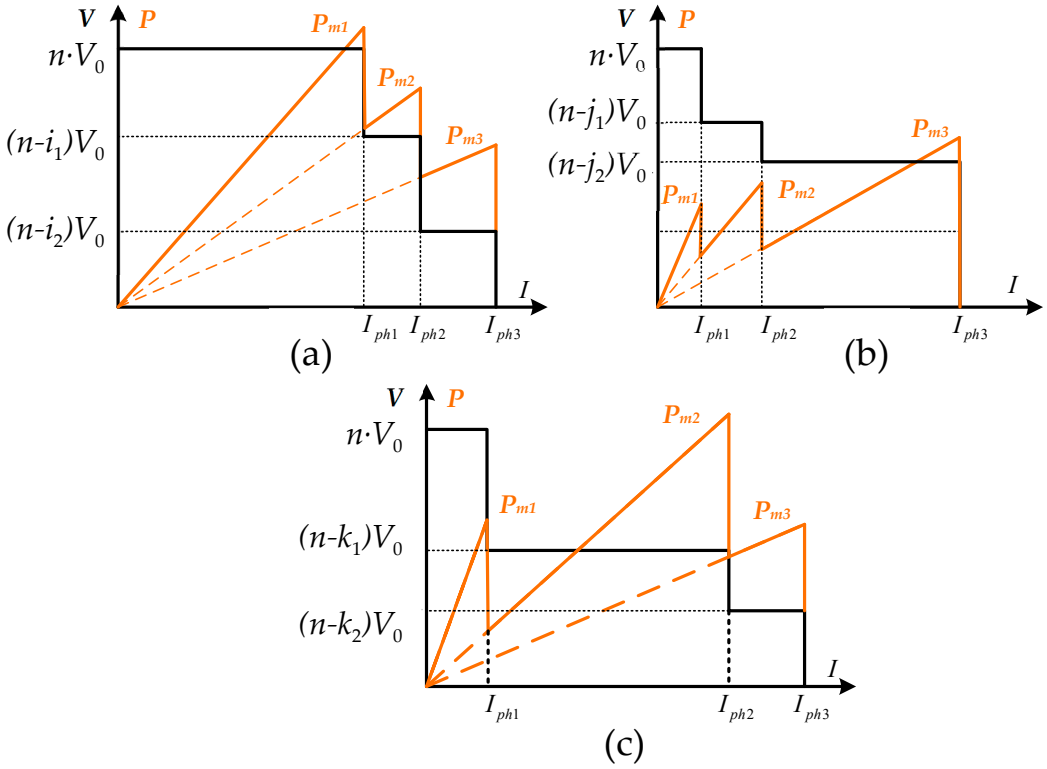

Figure 4. The *V–I* and *P–I* curves of a solar array with differently irradiated groups of modules: (**a**) the first maximum is the global one, (**b**) the third maximum is the global one, and (**c**) the second maximum is the global one.

For simplicity, three different irradiation conditions are considered: (i) Group of $n - i_1 - i_2$ modules are irradiated more strongly than other groups of modules; (ii) group of j_2 modules are irradiated more strongly than $n - j_2$ and j_1 groups of modules; and (iii) group of k_1 modules are irradiated more strongly than $n - k_1$ and k_2 groups of modules. The short-circuit current of any module or group of modules is higher when one is irradiated strongly than that of others. As bypass diodes are connected with each module hence *V–I* curves of this array are the combination of different rectangles. Initially, the voltage of the PV system is equal to the open-circuit voltage $[(V_{OC})_n = n \cdot V_{OC}]$ and remains unchanged with increasing current. In the present situation, all bypass diodes work as reverse bias mode; hence, the current does not flow through these diodes. Interestingly, this behavior changes meaningfully when the array current increases higher than I_{ph1}. The diodes of shaded (weakest/damaged) modules work in forward bias mode for further enhancement of current and a complementary current $[\approx I_P - I_{phn}]$ flows through these diodes. As a result, the voltage of the PV system drops down to the magnitude of $(n - i_1)V_{OC}$ (Figure 4a), $(n - j_1)V_{OC}$ (Figure 4b), and $(n - k_1)V_{OC}$ (Figure 4c). The voltage across the diode is smaller than that of the module, which can be neglected. Hereafter, the voltage of the PV system again remains constant with increasing current up to the next short-circuit current value I_{ph2}. The voltage of the PV system again decreases significantly to the magnitude of $(n - i_2)V_{OC}$ at the specific current I_{ph3} (Figure 4a). The voltage of the PV system drops down to zero if the current increases further. For other cases of irradiations, similar voltage changes are observed with different magnitudes of array current (Figure 4b,c). It is well-known that the generated electric power of the PV system and current have linear behavior for homogeneous radiation. The maximum power generation

is achieved at short-circuit current and is proportional to the magnitude of the voltage. The *V–I* curves have different slopes for differently irradiated modules of PV systems in case of partial shading. Accordingly, several maxima (local & global) exist in the *P–I* curves and each one is related to different slops in the voltage behavior of the PV system. The location of GM depends on short-circuit current and voltage outputs of the differently illuminated module or group of modules. For the present study, the GM is located at I_{ph1} for the first case (Figure 4a), at I_{ph3} for the second case (Figure 4b), and at I_{ph2} for the third one (Figure 4c).

2.4. Proposed Control Algorithm

The primary objective of the proposed algorithm is continuous control and monitoring of the regulating parameter. Figure 5 demonstrates the block diagram of the MPPT control algorithm to find the optimal value of regulating parameters during partial shading conditions. Let us assume that the well-known perturbation and observation (P&O) algorithm is employed [4]. The PV current is used as a regulating parameter, which is the most suitable parameter for this task, as stated previously [1]. Initially, the MPPT system starts to search maxima in the I–P curve by increasing PV current up to an optimal value. Simultaneously, the system continuously monitors the voltage and current of each PV module beginning from the open-circuit voltage (V_{OC}) of an entire string and (V_{OCn}) of each module when string current is equal to zero. Further equality of these stresses is assumed. At the same time, the upper and lower boundaries of regulating parameter are accurately determined using a soft procedure. The procedure of GM localization is as follows. First, diode current values of all diodes (D_1-D_n) are calculated using Equations (2)–(4). It is assumed that the module's temperature and parameters of an equivalent circuit of all modules are equal in the string. The module's temperature is permanently measured for the control MPPT system. Thus, voltages on diodes in equivalent circuits can be calculated as:

$$V_{D_n} = V_n + \left(I - I_{bpn}\right) \cdot R_{sn} \tag{6}$$

where V_n is the output voltage on the equivalent circuit of the PV module. Using V_{D_n}, the diode current is calculated as:

$$I_{D_n} = I_0\left[exp\left(\frac{q_e V_{D_n}}{a k_B T}\right) - 1\right] \tag{7}$$

The reverse saturation current of each module at every moment of time is calculated using Equation (2). Finally, photocurrents (I_{phn}) are estimated as:

$$I_{phn} = I - I_{D_n} - I_{bpn} \tag{8}$$

where I is the current of the entire string. Photocurrents are assumed to represent the upper boundaries of all maxima (local and global maximum). Therefore, all photocurrents are ranked from minimum to maximum value:

$$\left(I_p\right)_{min} < \ldots < \left(I_p\right)_{max} \tag{9}$$

The voltage magnitudes (V_j) associated with these photocurrents are estimated as:

$$V_j = V_{OC} - j \cdot V_{OCn} \tag{10}$$

where j is the serial number of photocurrents. It is assumed that the open-circuit voltages (V_{OCn}) of all individual modules are similar. Finally, all local maxima are determined as:

$$\left(P_m\right)_j = V_j \cdot \left(I_p\right)_j \tag{11}$$

which are ranked with the following finding of a GM between locals. The lower limit of this GM is assumed as 0.90–0.91 of its upper boundary in accordance with recommendations [19]. The optimal value of regulating parameter exists between these boundaries. During the process, the optimal value

is compared with its present magnitude. On the basis of this comparison, the algorithm decides to either persist at first maximum or to continuously increase the current toward the lower limit of the optimal value. If the algorithm decides to further increase the current up to the lower limit then conventional MPPT activates after achieving it. In this way, the MPPT system quickly finds the exact GM location. The PV current fluctuates around the optimal point until the location of GM is changed significantly. The algorithm decides to increase or decrease the optimal value of current according to the situation. Meanwhile, if the location of GM changes, then the MPPT algorithm switches-off and systems direct current toward the new location of GM. If the current value for the new GM location is higher as compared to the previous one, then the current increases toward the lower limit of the changed location. Instead, PV current decreases to the upper limit of the optimum value, if the new location of GM is lower than that of the previous one. When PV current achieves a new upper/lower boundary of optimal value, the MPPT system again switches on and promptly finds the location of the GM. This process continuously monitors the current and voltage of each PV module in order to concurrently estimate the upper and lower boundaries. A particular procedure calculates the upper and lower limits of regulating parameter using an equivalent circuit. The equivalent circuit of the module should be determined previously and included in the MPPT algorithm.

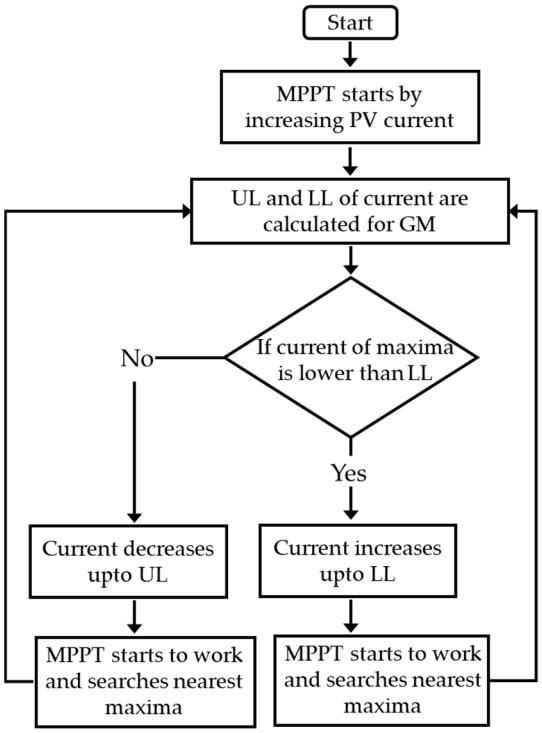

Figure 5. The maximum power point tracking (MPPT) algorithm to find the global maximum (GM) during the partial shading (UL is the upper limit, LL is the lower limit).

3. Results and Discussion

3.1. Simulation Studies

In order to verify the feasibility of the control algorithm and test the MPPT performance, simulation experiments on the system are performed using PSIM software. The schematic diagram of the proposed MPPT system is shown in Figure 6; this system works on the control algorithm as described in the previous section. This algorithm is based on conventional perturb and observe (P&O) approach. The schematic diagram of the control block of this system is shown in Figure 7. This system includes five serially connected modules, block to control regulating parameter, and block to estimate the location of the GM. As mentioned earlier, the primary function of regulating parameter is to find the exact location

of the GM and to stay at the same. At this moment, we consider that five PV modules connected serially; hence, this simulation is valid for any possible situation during partial shading. The simulation results of the proposed algorithm are demonstrated in Figure 8.

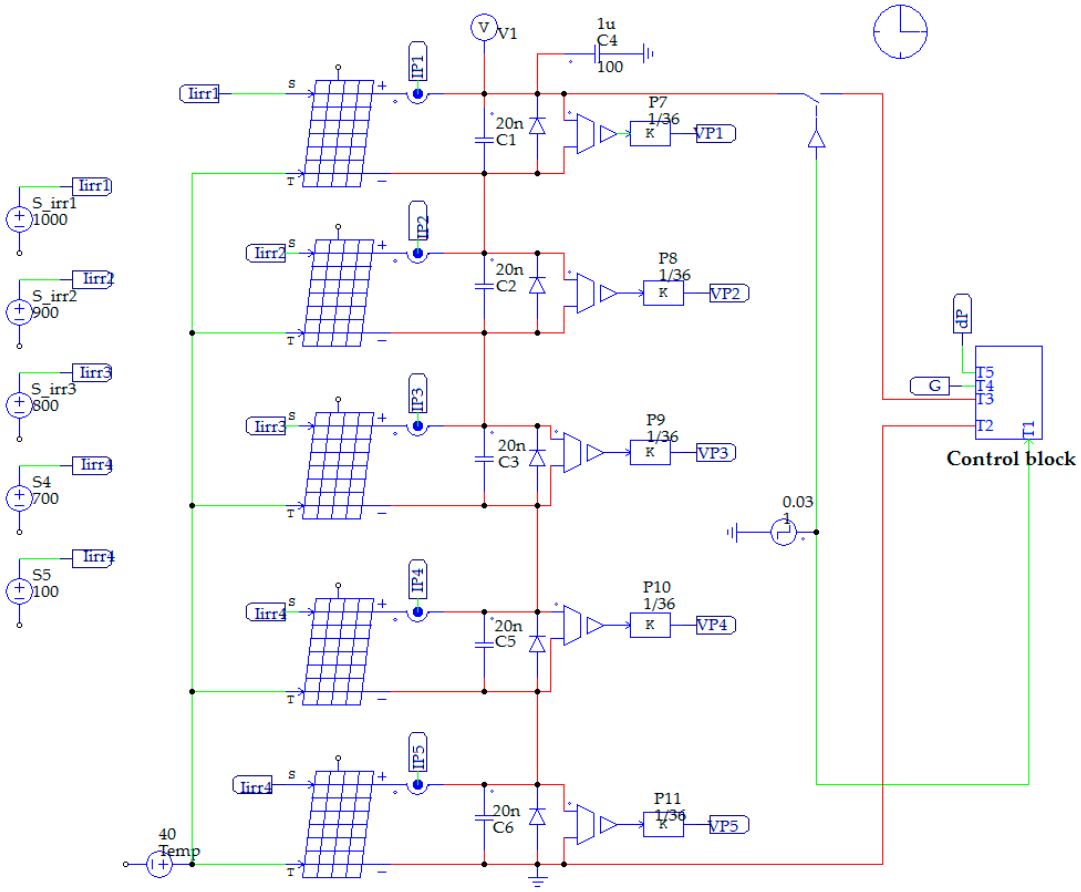

Figure 6. The PSIM circuit for MPPT control.

During the search process, the MPPT finds two maxima one is at ~0.025 s and another one is at ~0.13 s (Figure 8a). It is observed that the system neglects all local maxima and achieves the exact location of GM very rapidly (0.12–0.17 s). The proposed algorithm directly leads the controller current to the vicinity of the GM and applies the well-known P&O scheme. The PV system works typically if the solar irradiance does not change and the current of PV modules remains in the defined range. The location of GM changes significantly in the case of partial shading conditions or variable solar irradiance. The proposed algorithm directs the MPPT system to change the PV module current to inside new limits according to the situation. Note: Any conventional MMPT method can be utilized with this algorithm. Figure 8b shows the relation between output power and GM search time at different temperatures (30 °C, 40 °C, 50 °C, and 60 °C).

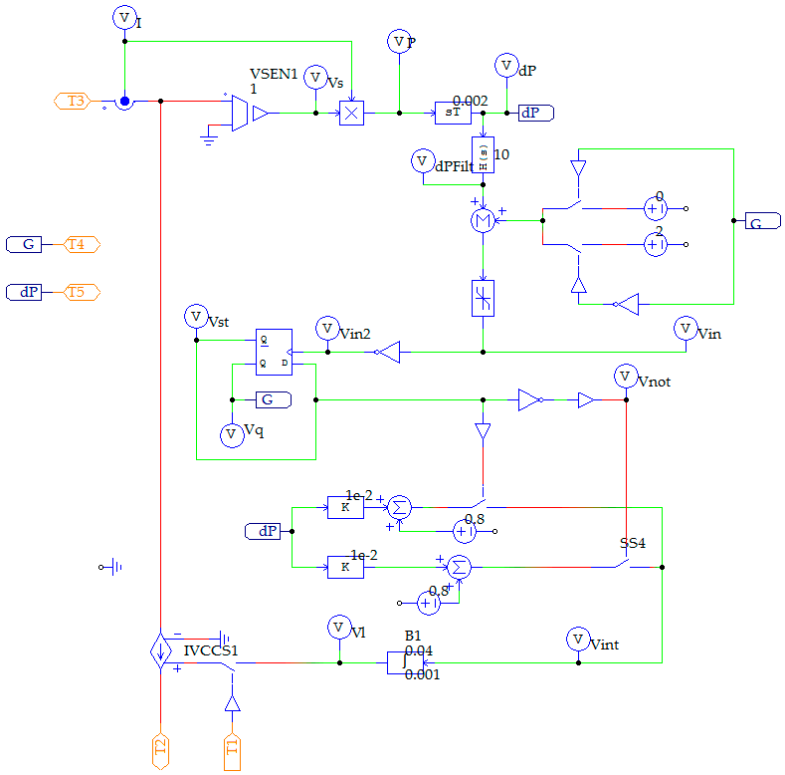

Figure 7. Control block of the PSIM circuit for MPPT control (Figure 6).

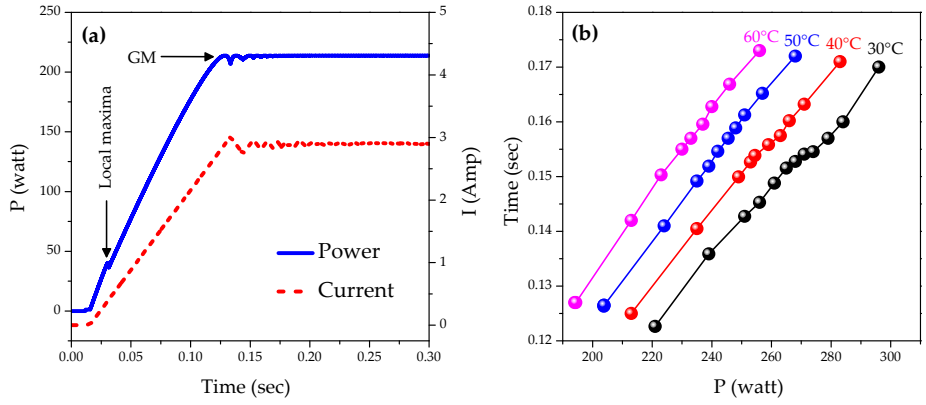

Figure 8. (**a**) The power and current as a function of time during MPPT functioning in order to find the GM in partial shading; (**b**) the GM search time as a function of power at different temperatures.

3.2. Efficiency of the Algorithm

One of the significant differences between this method than that of others is the selection of module current as of the regulating parameter, which improves control sustainability. This method regularly monitors PV characteristics of each module and simultaneously implements a simplified equivalent circuit to find GM location. The efficiency of any algorithm MPPT can be estimated by the comparison of a search time required for an algorithm achieving GM. Table 1 summarizes the data of search time for different algorithms. It is found that P&O and INC techniques are faster than that of the proposed algorithm. However, these algorithms are suitable in the case of a homogeneous solar irradiance. These algorithms may be lost GM or even do not find it at the beginning of the MPPT application during partial shading.

Table 1. Comparison between search time for different MPPT techniques.

Type of Algorithm		Search Time (s)	Ref.
Conventional searching algorithms	Perturbation and observation (P&O)	0.04–0.08	[16,42]
	Incremental conductance (INC)	0.03–0.05	[42]
Inspired by Nature or Bio-organisms	Particle swam optimization (PSO)	1–2	[23]
	Cuckoo search algorithm (CSA)	1–2	[43]
	Artificial bee colony (ABC)	0.4–2	[44]
	Grey wolf optimization technique	1–2	[25]
Stochastic adapting search	Transfer reinforcement learning (TRL)	1–1.5	[34]
	Monte-Carlo	1–3	[45]
Mathematical Modeling	Proposed	0.12–0.17	

Last but not least, the mathematical results are not precise, but the essence of our conclusions on maximum localizations remains correct and close to real conditions. More importantly, the tracking time can be diminished by up to 0.12–0.17 s by the optimal design of the current controller. The efficiency and accuracy of the proposed algorithm may be similar to other conventional methods. However, both parameters are consistent for shorter tracking

4. Conclusions

In this article, an efficient maximum power point tracking (MPPT) algorithm was proposed to achieve global maxima (GM) during partial fast-shading conditions and variable solar radiation. This algorithm was based on the simplified equivalent circuit of the PV module. In the process, mathematical modeling was performed on the measured module parameters. The functionality of the proposed algorithm was verified using the PSIM simulation software. At the first step, the lower and upper boundaries of the GM were precisely determined by the MPPT controller. All local maxima were ignored in this process. Later, conventional algorithms (P&O or incremental conductance methods) were applied to find the exact location of GM.

More importantly, the MPPT system continuously monitored the PV parameters and determined the GM boundaries accordingly. If the system found any changes in the GM location, then MPPT moved toward a new location instantly. Simulation results showed that this system was fast enough to determine the GM location than that of other methods for partial shading conditions. The efficiency of the proposed algorithm is 6–8 times better than that of the bio- or natural inspired algorithms. The proposed algorithm is suggested to use for industrial MPPT systems, which aims to work on high voltage PV strings. Such MPPT systems can improve solar electricity production up to a higher level. The proposed algorithm is the best choice for MPPT techniques during partial shading conditions and non-uniform solar irradiance.

Author Contributions: Conceptualization: M.A., S.R. and A.Y.; methodology: S.R., M.A. and T.M.; formal analysis, S.R. and M.A.; investigation, S.R.; writing—original draft preparation, S.R., T.M. and M.A.; writing—review and editing, M.A. and A.Y.; supervision, M.A. and A.Y.

Funding: This research received no external funding.

Acknowledgments: Shailendra Rajput is thankful to the Israeli Council for Higher Education (CHE) for fellowship.

Conflicts of Interest: The authors declare no conflict of interest.

Abbreviations

The following abbreviations and nomenclature are used in this manuscript:

MPPT	Maximum power point tracking
PV	Photovoltaic
GM	Global maximum
GMPP	Global maximum power point
P&O	Perturbation-observation
PSO	Particle swarm optimization

DE	Differential evolutionary
DEPSO	Combination of DE and PSO algorithms
GWO	Grey wolf optimization
SA	Simulated annealing
INC	Incremental conductance
ABC	Artificial bee colony
CSA	Cuckoo search algorithm
TRL	Transfer reinforcement learning
V-I	Voltage-current
P-I	Power-current
I_{ph}	Photocurrent
I_0	Reverse saturation current
a	Module quality factor
k_B	Boltzmann constant
q_e	Elementary charge
T	Cell/module temperature
V_T	Thermal voltage
T_{ref}	Reference temperature (300 K)
E_g	Band gap
S	Solar irradiation level
J_0	Temperature coefficient
$(I_{SC})_0$	I_{SC} at a reference temperature
D	Diode
I_D	Diode current
V_D	Diode voltage
R_{sh}	Shunt resistance
I_{sh}	Shunt current
R_S	Series resistance
I	Output current
V_0	Output voltage
V_{OC}	Open-circuit voltage
V_{OCn}	Open-circuit voltage of individual PV module
I_{SC}	Short-circuit current
D_{bp}	Bypass diode
I_{bp}	Bypass diode current
V_{array}	Voltage of n-serially connected PV modules
UL	Upper limit
LL	Lower limit

References

1. Zsiborács, H.; Hegedűsné Baranyai, N.; Csányi, S.; Vincze, A.; Pintér, G. Economic Analysis of Grid-Connected PV System Regulations: A Hungarian Case Study. *Electronics* **2019**, *8*, 149. [CrossRef]
2. REN21. *Renewables 2019 Global Status Report—REN21*; REN21: Paris, France, 2019.
3. Doshi, Y. Solar Photovoltaic (PV) Panels Market Overview. Available online: https://www.alliedmarketresearch.com/solar-photovoltaic-panel-market (accessed on 12 September 2019).
4. Bahar, H. Tracking Clean Energy Progress. Available online: https://www.iea.org/tcep/power/renewables/solarpv/ (accessed on 12 September 2019).
5. Du, Y.; Yan, K.; Ren, Z.; Xiao, W. Designing Localized MPPT for PV Systems Using Fuzzy-Weighted Extreme Learning Machine. *Energies* **2018**, *11*, 2615. [CrossRef]
6. Belhachat, F.; Larbes, C. Comprehensive review on global maximum power point tracking techniques for PV systems subjected to partial shading conditions. *Sol. Energy* **2019**, *183*, 476–500. [CrossRef]
7. Zhang, M.; Chen, Z.; Wei, L. An Immune Firefly Algorithm for Tracking the Maximum Power Point of PV Array under Partial Shading Conditions. *Energies* **2019**, *12*, 3083. [CrossRef]

8. Zhang, Y.; Zhu, J.; Dong, X.; Zhao, P.; Ge, P.; Zhang, X. A Control Strategy for Smooth Power Tracking of a Grid-Connected Virtual Synchronous Generator Based on Linear Active Disturbance Rejection Control. *Energies* **2019**, *12*, 3024. [CrossRef]
9. Yahalom, A.; Tatiana, M.; Averbukh, M. Modified approach for global MPP finding under partial shading. In Proceedings of the 2018 IEEE International Conference on the Science of Electrical Engineering (ICSEE), Eilat, Israel, 12–14 December 2018; pp. 1–5.
10. Zhu, Y.; Kim, M.K.; Wen, H. Simulation and Analysis of Perturbation and Observation-Based Self-Adaptable Step Size Maximum Power Point Tracking Strategy with Low Power Loss for Photovoltaics. *Energies* **2019**, *12*, 92. [CrossRef]
11. Bataineh, K.; Eid, N. A Hybrid Maximum Power Point Tracking Method for Photovoltaic Systems for Dynamic Weather Conditions. *Resources* **2018**, *7*, 68. [CrossRef]
12. Killi, M.; Samanta, S. Modified perturb and observe MPPT algorithm for drift avoidance in photovoltaic systems. *IEEE Trans. Ind. Electron.* **2015**, *62*, 5549–5559. [CrossRef]
13. Kumar, N.; Hussain, I.; Singh, B.; Panigrahi, B.K. Self-Adaptive Incremental Conductance Algorithm for Swift and Ripple-Free Maximum Power Harvesting from PV Array. *IEEE Trans. Ind. Inform.* **2018**, *14*, 2031–2041. [CrossRef]
14. Averbukh, M.; Ben-Galim, Y.; Uhananov, A. Development of a quick dynamic response maximum power point tracking algorithm for off-grid system with adaptive switching (On–Off) control of dc/dc converter. *J. Sol. Energy Eng.* **2013**, *135*, 021003. [CrossRef]
15. Pahari, O.P.; Subudhi, B. Integral sliding mode-improved adaptive MPPT control scheme for suppressing grid current harmonics for PV system. *IET Renew. Power Gen.* **2018**, *12*, 1904–1914. [CrossRef]
16. Karabacak, M. A new perturb and observe based higher order sliding mode MPPT control of wind turbines eliminating the rotor inertial effect. *Renew. Energy* **2019**, *133*, 807–827. [CrossRef]
17. Bouarroudj, N.; Boukhetala, D.; Feliu-Batlle, V.; Boudjema, F.; Benlahbib, B.; Batoun, B. Maximum Power Point Tracker Based on Fuzzy Adaptive Radial Basis Function Neural Network for PV-System. *Energies* **2019**, *12*, 2827. [CrossRef]
18. Macaulay, J.; Zhou, Z. A Fuzzy Logical-Based Variable Step Size P&O MPPT Algorithm for Photovoltaic System. *Energies* **2018**, *11*, 1340. [CrossRef]
19. Yahalom, A.; Domorad, P.; Averbukh, M. New approach for localization global maximum of solar array. In Proceedings of the 2017 19th European Conference on Power Electronics and Applications (EPE'17 ECCE Europe), Warsaw, Poland, 11–14 September 2017; pp. 1–10.
20. Li, Y.; Li, X.; Liu, J.; Ruan, X. An Improved Bat Algorithm Based on Lévy Flights and Adjustment Factors. *Symmetry* **2019**, *11*, 925. [CrossRef]
21. Li, H.; Yang, D.; Su, W.; Lü, J.; Yu, X. An Overall Distribution Particle Swarm Optimization MPPT Algorithm for Photovoltaic System Under Partial Shading. *IEEE Trans. Ind. Electron.* **2019**, *66*, 265–275. [CrossRef]
22. Garcia-Guarin, J.; Rodriguez, D.; Alvarez, D.; Rivera, S.; Cortes, C.; Guzman, A.; Bretas, A.; Aguero, J.R.; Bretas, N. Smart Microgrids Operation Considering a Variable Neighborhood Search: The Differential Evolutionary Particle Swarm Optimization Algorithm. *Energies* **2019**, *12*, 3149. [CrossRef]
23. Rajendran, S.; Srinivasan, H. Simplified accelerated particle swarm optimization algorithm for efficient maximum power point tracking in partially shaded photovoltaic systems. *IET Renew. Power Gen.* **2016**, *10*, 1340–1347. [CrossRef]
24. Song, Y.; Hu, W.; Xu, X.; Huang, Q.; Chen, G.; Han, X.; Chen, Z. Optimal Investment Strategies for Solar Energy Based Systems. *Energies* **2019**, *12*, 2826. [CrossRef]
25. Mohanty, S.; Subudhi, B.; Ray, P.K. A New MPPT Design Using Grey Wolf Optimization Technique for Photovoltaic System Under Partial Shading Conditions. *IEEE Trans. Sustain. Energy* **2016**, *7*, 181–188. [CrossRef]
26. Lyden, S.; Haque, M.E. A Simulated Annealing Global Maximum Power Point Tracking Approach for PV Modules Under Partial Shading Conditions. *IEEE Trans. Power Electron.* **2016**, *31*, 4171–4181. [CrossRef]
27. Seyedmahmoudian, M.; Rahmani, R.; Mekhilef, S.; Oo, A.M.T.; Stojcevski, A.; Soon, T.K.; Ghandhari, A.S. Simulation and Hardware Implementation of New Maximum Power Point Tracking Technique for Partially Shaded PV System Using Hybrid DEPSO Method. *IEEE Trans. Sustain. Energy* **2015**, *6*, 850–862. [CrossRef]
28. Chen, K.; Tian, S.; Cheng, Y.; Bai, L. An Improved MPPT Controller for Photovoltaic System Under Partial Shading Condition. *IEEE Trans. Sustain. Energy* **2014**, *5*, 978–985. [CrossRef]

29. Li, X.; Wen, H.; Hu, Y.; Jiang, L.; Xiao, W. Modified Beta Algorithm for GMPPT and Partial Shading Detection in Photovoltaic Systems. *IEEE Trans. Power Electron.* **2018**, *33*, 2172–2186. [CrossRef]
30. Pathy, S.; Subramani, C.; Sridhar, R.; Thamizh Thentral, T.M.; Padmanaban, S. Nature-Inspired MPPT Algorithms for Partially Shaded PV Systems: A Comparative Study. *Energies* **2019**, *12*, 1451. [CrossRef]
31. Alshareef, M.; Lin, Z.; Ma, M.; Cao, W. Accelerated particle swarm optimization for photovoltaic maximum power point tracking under partial shading conditions. *Energies* **2019**, *12*, 623. [CrossRef]
32. Huang, Y.P.; Ye, C.E.; Chen, X. A Modified Firefly Algorithm with Rapid Response Maximum Power Point Tracking for Photovoltaic Systems under Partial Shading Conditions. *Energies* **2018**, *11*, 2284. [CrossRef]
33. Seyedmahmoudian, M.; Kok Soon, T.; Jamei, E.; Thirunavukkarasu, G.S.; Horan, B.; Mekhilef, S.; Stojcevski, A. Maximum Power Point Tracking for Photovoltaic Systems under Partial Shading Conditions Using Bat Algorithm. *Sustainability* **2018**, *10*, 1347. [CrossRef]
34. Ding, M.; Lv, D.; Yang, C.; Li, S.; Fang, Q.; Yang, B.; Zhang, X. Global Maximum Power Point Tracking of PV Systems under Partial Shading Condition: A Transfer Reinforcement Learning Approach. *Appl. Sci.* **2019**, *9*, 2769. [CrossRef]
35. Gosumbonggot, J.; Fujita, G. Partial shading detection and global maximum power point tracking algorithm for photovoltaic with the variation of irradiation and temperature. *Energies* **2019**, *12*, 202. [CrossRef]
36. Power Optimizer. Available online: https://www.solaredge.com/us/pv-professionals (accessed on 11 September 2019).
37. Special Benefit Based on Smart DC Module. Available online: https://krannich-solar.com/en/service/about-solar-power.html (accessed on 11 September 2019).
38. Lineykin, S.; Averbukh, M.; Kuperman, A. An improved approach to extract the single-diode equivalent circuit parameters of a photovoltaic cell/module. *Renew. Sustain. Energy Rev.* **2014**, *30*, 282–289. [CrossRef]
39. Majdoul, R.; Abdelmounim, E.; Aboulfatah, M.; Touati, A.W.; Moutabir, A.; Abouloifa, A. Combined analytical and numerical approach to determine the four parameters of the photovoltaic cells models. In Proceedings of the 2015 International Conference on Electrical and Information Technologies (ICEIT), Marrakech, Morocco, 25–27 March 2015; pp. 263–268.
40. Lineykin, S.; Averbukh, M.; Kuperman, A. Issues in modeling amorphous silicon photovoltaic modules by single-diode equivalent circuit. *IEEE Trans. Ind. Electron.* **2014**, *61*, 6785–6793. [CrossRef]
41. Varshni, Y.P. Temperature dependence of the energy gap in semiconductors. *Physica* **1967**, *34*, 149–154. [CrossRef]
42. Bouselham, L.; Hajji, B.; Hajji, H. Comparative study of different MPPT methods for photovoltaic system. In Proceedings of the 2015 3rd International Renewable and Sustainable Energy Conference (IRSEC), Marrakech, Morocco, 10–13 December 2015; pp. 1–5.
43. Nugraha, D.A.; Lian, K.L. A Novel MPPT Method Based on Cuckoo Search Algorithm and Golden Section Search Algorithm for Partially Shaded PV System. *Can. J. Elect. Comput. E* **2019**, *42*, 173–182.
44. Li, N.; Mingxuan, M.; Yihao, W.; Lichuang, C.; Lin, Z.; Qianjin, Z. Maximum Power Point Tracking Control Based on Modified ABC Algorithm for Shaded PV System. In Proceedings of the 2019 AEIT International Conference of Electrical and Electronic Technologies for Automotive (AEIT AUTOMOTIVE), Torino, Italy, 2–4 July 2019; pp. 1–5.
45. Chen, L.; Wang, X. An Enhanced MPPT Method based on ANN-assisted Sequential Monte Carlo and Quickest Change Detection. *arXiv* **2018**, arXiv:1805.04922. [CrossRef]